Is there Information in Residuals: Hydrograph and Recession Flows Predictions using Deep Learning?

Abhinav Gupta[1*] and Sean A. McKenna[2]

[1]Department of Chemical and Environmental Engineering, University of Cincinnati, Cincinnati, OH

[2]Division of Hydrologic Sciences, Desert Research Institute, Reno, NV

Corresponding author: Abhinav Gupta (abhigupta.1611@gmail.com)

*Department of Chemical and Environmental Engineering, 2600 Clifton Ave., University of Cincinnati, Cincinnati, OH 45221

Highlights

1. Adding global model outputs as input to a locally trained model can improve streamflow simulation accuracy.
2. Recession flow simulation may be improved by combining global and local information.
3. Watershed uniqueness has significant control over global model performance.

This peer-print has not been peer-reviewed.

Abstract

This study examines streamflow simulations using deep learning (DL) to: (1) Understand why global DL models trained on multiple watersheds outperform local DL models trained on single watersheds, given the watershed uniqueness hypothesis and (2) Improve recession flow simulation accuracy. It introduces a novel global-local (GL) modeling strategy, where global model outputs are fed as input to a locally trained model, with the hypothesis that this strategy can leverage both global and watershed-specific information. GL models demonstrate enhanced accuracy in recession flow prediction for 30% of the watersheds compared to global and local models. However, considering the entire hydrograph, GL models often perform worse than the global model. Our results suggest that watershed uniqueness play a significant role in the performance of global models, suggesting that even global LSTM models should be tailored to individual watersheds.

Plain language summary

This study presents a new way to generate computer simulations of streamflow by using deep learning methods. The main idea is to use a learning model to extract information from many different watersheds and to also learn unique details of each watershed. An example of unique details include errors in data (rainfall and streamflow) that are watershed specific. This new approach improves the accuracy of streamflow predictions in some watersheds during recession post-rainfall, but it does not work as well across entire history of streamflow in which case a model built with information from all watersheds is superior. We hypothesized that watershed uniqueness, for example, in the form of the errors in measuring the rainfall and streamflow data, have a large impact on performance of the different models. Models trained with data from many watersheds are not as affected by these errors as strongly as models trained with data from just one watershed. This study shows the importance of accounting for errors in the data when building computer simulations of streamflow.

1. Introduction

Several rainfall-runoff models have been used for streamflow simulation including conceptual and process-based (PB) hydrological models (Singh, 1995), statistical time series models (Beven, 2011), machine learning (ML; Govindaraju, 2000) including deep learning models (DL; Shen & Lawson, 2021). For any approach, model parameters must be calibrated/trained to match the model output with the available data which is typically streamflow time series. Each watershed is unique with respect to details of the rainfall-runoff processes and in terms of errors in hydrological data (Beven, 2000, 2020). In the context of rainfall-runoff modeling, hydrological data include meteorological data such as precipitation and temperature, streamflow data and watershed static attributes. Because of the uniqueness of place, it is a common practice to calibrate rainfall-runoff models on data available within a single watershed where predictions are required.

A DL model trained on data across multiple watersheds (referred to as a global model in this study) typically outperforms DL models trained on single watersheds (referred to as local models; Nearing et al., 2021; Li et al., 2022). One reason that global DL models outperform the locally calibrated DL models may be the extra hydrological information available to the global DL models through data across different watersheds (Kratzert et al., 2019; Gauch et al., 2021; Nearing et al., 2021). Another reason for the improved performance may be that local, watershed-specific, *nonstationary* errors in hydrological data can degrade the performance of local DL models because a local DL model will fit these systematic errors while the global DL model will average out these errors (Beven, 2023). In this paper, the term nonstationarity is used in the sense discussed by Beven (2016). According to this definition, a given time series can be treated as nonstationary if its statistical properties change with time or its length is too small to robustly estimate the statistical properties. For example, errors associated with 3-10 return-year event may not be well characterized by 10-20 years of calibration data. Presence of nonstationarities in the residuals between observed and model predicted streamflows is well established in hydrological community (Nearing, 2014; Smith et al., 2015; Ammann et al., 2019).

Ideally, a DL model would extract all the information about streamflow from the available data. In practice, however, this may not happen because of uniqueness of watersheds. For example, the choice of model hyperparameters can significantly affect the amount of information extracted from the training data of a watershed. Therefore, one can expect the residuals between observed and global model-predicted streamflow would have some systematic structure, at least for some watersheds. In this study, we investigate whether there is any *learnable* structure in these residuals. To this end, we propose a simple strategy that combines global and local modeling approaches to predict streamflow. The benefit of this strategy is that streamflow simulations can be more accurate than the ones simulated by a global model if there is any watershed-specific learnable structure in the residuals. Thus, the first objective of this study was to test a new DL modeling strategy to combine global and local information for streamflow simulation, that can take advantage of both the ability of a global model to generalize across variability in multiple watersheds and the potential information available in the form of local errors in the hydrological data of a watershed. The proposed DL strategy is an attempt to extract meaningful information from the residuals between observed streamflows and the global model-predicted streamflows. Specifically, this study (1) provides insight into why the global DL models perform better than the locally trained DL models, and (2) explores whether the streamflow simulation performance can be improved by the global-local strategy.

Previous studies have focused on the prediction of entire streamflow hydrographs using ML/DL (e.g., Ma et al., 2021; Li et al., 2022). This may result in suboptimal predictions of the recession flows (Knoben et al., 2020; Gupta, 2024). Therefore, the second objective of this study was to explore separate modeling of recession flows and full hydrograph.

2. Deep learning (DL) models

A long short-term memory (LSTM) network is used as the basic DL model as it has been shown to yield state-of-the-art performance in streamflow simulations (Nearing et al., 2021). Details of the LSTM can be found in Kratzert et al. (2019) and Goodfellow et al. (2016). A single LSTM layer with 128 neurons was used in this study. Four types of models were trained (Figure 1): (1) A separate model for each watershed such that streamflow in a watershed was predicted using the LSTM model trained only on data from that watershed (local model) (2) Trained using data from all the watersheds (global model), (3) A combination of global and local models where the output of a global model is appended with meteorological data and is passed through a local model (GL0 model), and (4) a combination of global and local models where the output of the global model is used as the sole input to the local model (GL1 model). The difference between GL0 and GL1 models is that meteorological data are (not) fed to the local component in GL0

(GL1) model. This allowed us to test whether the remaining information in the residuals between global model predicted and observed streamflows is dependent upon the meteorological data. In Figure 1, the symbol X_t denotes the meteorological data varying with time t including precipitation, minimum and maximum temperatures, vapor pressure, and solar radiation. The symbol S denotes static attributes (see Addor et al., 2017a) including soil and geological properties, topographical data, and the long-term climate of a watershed. The symbol k denotes the length of past meteorological data used as input to the LSTM. Further, each of the four models was trained separately using data for both the entire hydrograph and data for recession flows only. Recession flows were defined as the flows during which rainfall was below $0.1\ \mathrm{mm/day}$, beginning at least three days after the preceding peak streamflow (see Figure S1 in supplementary information (SI)).

The value of k was set to 365 days for the 'entire hydrograph models' and 60 days for the 'recession flow models'. The value of $k = 60$ day was deemed sufficient for recession flows as increasing it further did not improve the performance. Kim et al. (2023) used $k = 10$ where they considered a single watershed for recession flow modeling. In this study, Nash-Sutcliff Efficiency (NSE; Nash & Sutcliffe, 1970) in the form suggested by Kratzert et al., (2019) was used as a performance metric and the objective function to be maximized during model training. Other LSTM hyper-parameters used in this study are described in the Text S2 (SI). The performance of the models was also assessed using Kling-Gupta efficiency (KGE) but the results were quite similar to the ones with NSE values; therefore, KGE results are shown in SI (Figures S2 and S3) only. Further, the models were also trained using normalized mean absolute error (NMAE, see Eq. (S1) in SI) as the objective function, these results are also shown in SI (Figures S5 and S6). The separate models for recession flow periods were trained by giving a weight of 1 to all the recession flow time steps and a weight of 0 to other time steps. The training period for all the models was 1980-1989 water years, the validation period was 1990-1994 water years, and the testing period was 2001-2013 years. Simulated daily mean streamflow is the output of each model.

3. Data

The Catchment Attributes and Meteorology for Large Sample Studies (CAMELS; Addor et al., 2017a, 2017b; Newman et al., 2014, 2015) dataset was used to develop different models. The CAMELS dataset contains daily timescale hydrometeorological and catchment attribute data from 671 watersheds across the USA (Addor et al., 2017a). All the CAMELS watersheds are free of anthropogenic disturbances (Kratzert et al., 2019); therefore, the results and conclusions presented in this paper are not influenced by these disturbances. In this study, 210 watersheds that were primarily driven by rainfall were used. These 210 watersheds (see Figure 4 below) cover most of the geographical regions of the USA and have different hydroclimatic conditions.

The global model was trained on training data from all the 210 watersheds that was then used to predict streamflow for all the watersheds in the testing period. Local models were trained on data from individual watersheds: Each local model was trained on training data from a single watershed and was used to predict streamflow in the testing period only in that watershed. Similarly, there were 210 GL0 and GL1 models, one GL0 and GL1 model for each watershed.

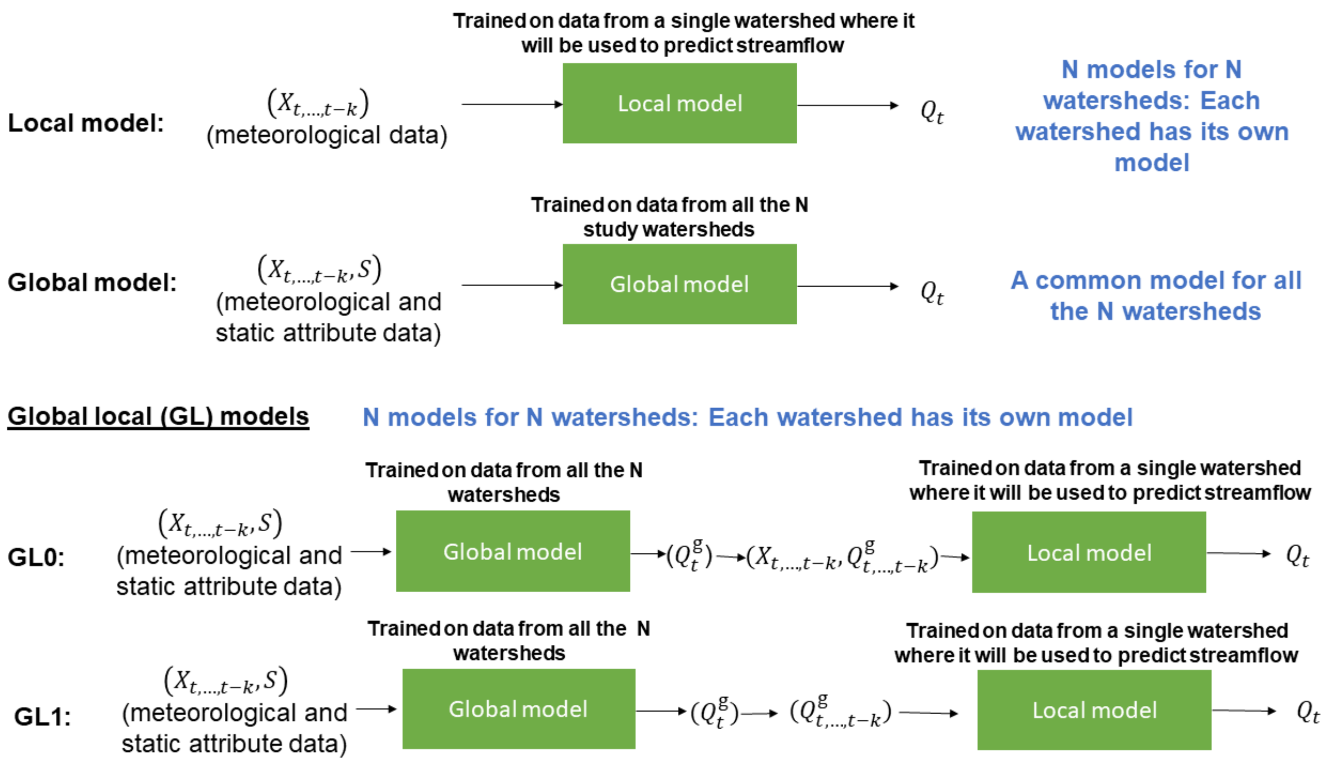

Figure 1. Illustrative description of the four models. Q_t denotes the final predicted streamflow in all the models and $Q_{t,\ldots,t-k}^g$ denotes the streamflow predicted by global models in the two global-local (GL) models at current time-step and past k time-steps. See the main text for the description of other symbols.

4. Comparison of model performance

Global models outperformed the other three models in predicting the entire hydrograph (Figures 2a and 2b). Local models performed the worst; the GL0 and GL1 models performed better than the local models. In most watersheds, the global model outperformed the local models, below the 1:1 line in Figure 2c, but there were a few watersheds for which the local models were better. GL0 and GL1 models performed similarly to the global model for a large number of watersheds (Figures 2d and 2e) but performed worse in several others. The GL1 model performed slightly better than GL0 model for most of the watersheds, with a significant difference in performance for a few watersheds (Figure 2f). These results indicate that the global modeling strategy is the best (or at least as good as other strategies) for nearly all watersheds when the model is trained for the entire hydrograph and evaluated using NSE. However, it is important to note that local and GL models did perform better than the global model for a few watersheds, implying that the global model could not extract all the available information during the training phase.

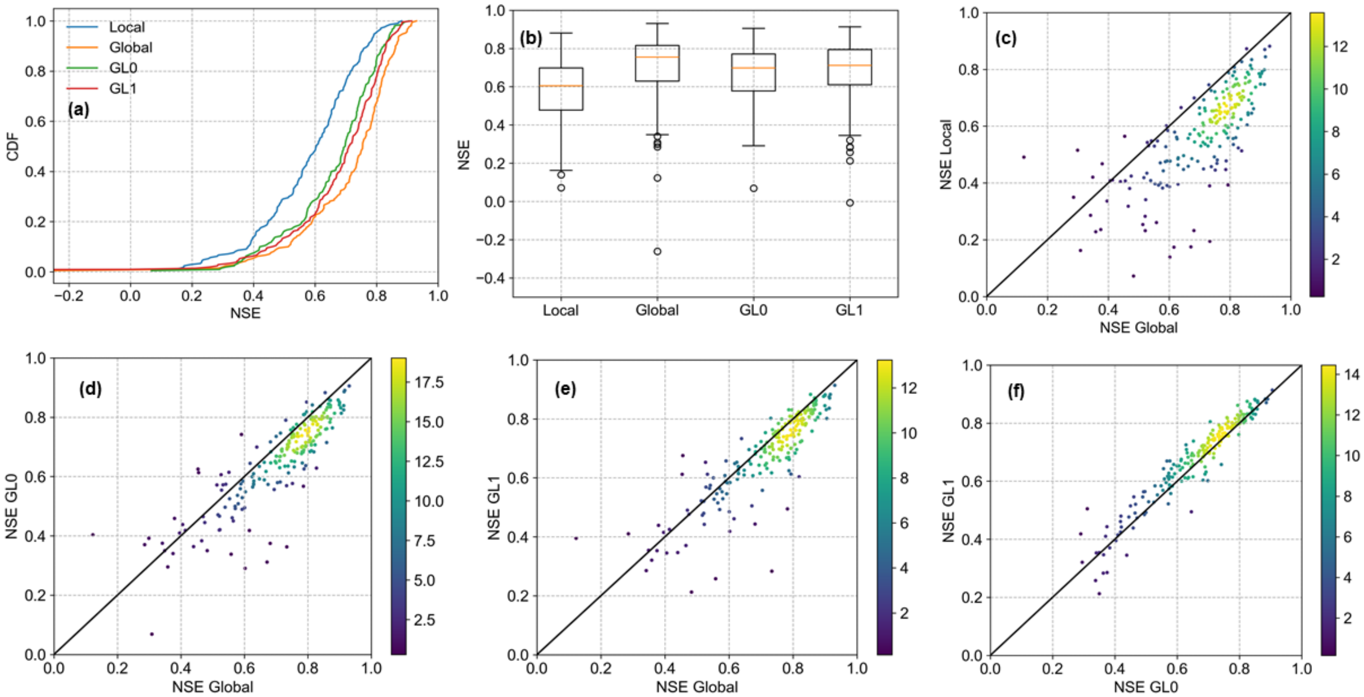

Figure 2. Entire hydrograph models. **(a)** Cumulative distribution function (CDF) and **(b)** boxplots of NSEs, the model with smaller area under its CDF is a better model. **(c), (d), (e), and (f)** Scatter plots of NSEs obtained by different models where x and y axes are clipped at 0.

When the models were trained to predict recession flows, no clear best strategy emerged (Figure 3). Local models performed worse than the other three models for most watersheds but there were many watersheds where local models performed better than the global model (Figure 3c). However, in most of the cases where the local models were better, recession flow predictability was low ($NSE \leq 0.50$). Similarly, the GL models outperformed the global model for $\approx 30\%$ of the watersheds where recession flow predictability was low ($NSE < 0.55$ approximately, Figures 3a, 3c, and 3d). Conversely, the global model outperformed GL models in watersheds where the global model NSE values were high (> 0.70 approximately). We conclude that the best model for recession flow depends upon the watershed being considered. Another noteworthy point is that GL0 and GL1 models yielded large improvement over the global model in some of the watersheds. Thus, postprocessing of the global model predicted streamflow, as is done here, is a viable strategy for recession flow predictions, depending upon the watershed being considered. The difference between the performance of GL0 and GL1 models depended strongly upon the watershed: GL0 performed better for some watersheds, while GL1 performed better for the others.

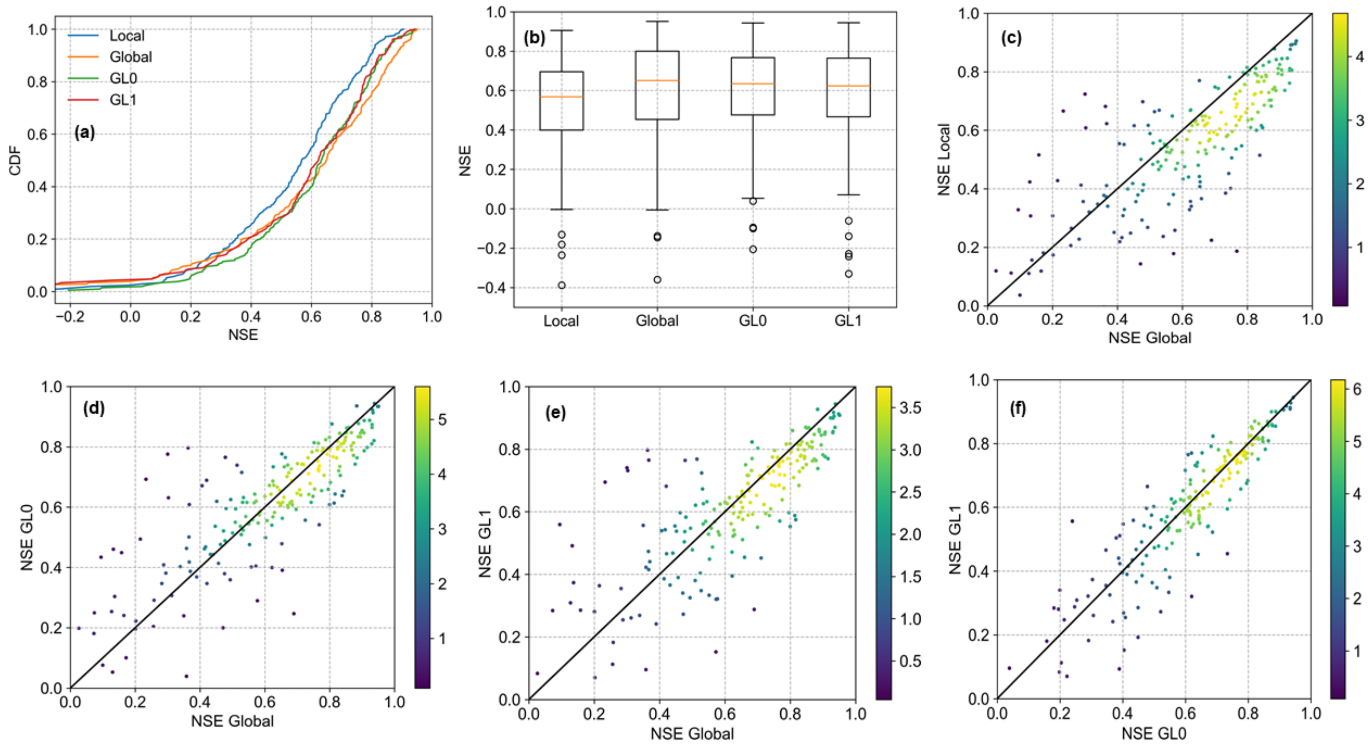

Figure 3. Same as Figure 2 but for recession flow models.

To further understand the utility of the GL modeling strategy for recession flows, each watershed was categorized into one of four categories based on GL model performance relative to the global model performance as listed below:

(a) Category 1: At least one GL model improves the performance by NSE of 0.05 while the other model does not change the performance,
(b) Category 2: At least one GL model worsens the performance by NSE of 0.05 while the other model does not change the performance,
(c) Category 3: No change in performance by any model (NSE of the models within ± 0.05)
(d) Category 4: One of the GL models improves the performance by NSE of 0.05 while the other worsens the performance by NSE of 0.05

Figure 4a shows the locations of the categories of watersheds. There were several watersheds, especially in the eastern USA, that belonged to category 1 where the GL modeling strategy significantly improved the performance for recession flows. Also, many watersheds belonged to category 2 where GL models degraded the performance. Therefore, we conclude that in several watersheds (category 1) the GL modeling strategy is better compared to either global or local modeling strategies as it allows the model to learn from both the hydrological information contained in the donor watersheds and the local information in the parent watershed. But the watersheds where GL models performed better than the global model were scattered in space without any spatial structure. Absence of a spatial structure in Figure 4a indicates that the improved performance of GL models over global model is not explainable by watershed characteristics or climatological properties as these properties are continuous in space in CAMELS dataset (see Addor et al., 2017a). This suggests that unique characteristics of watersheds may be playing a significant role in determining the ability of the global model to extract information and performance of GL modeling strategy. A few watersheds belonged to category 3 where any of the GL models did not result in any significant change in performance compared to the global model. Only four watersheds belonged to category 4 where the one GL model significantly improved while the other GL model significantly worsened the performance relative to the global model.

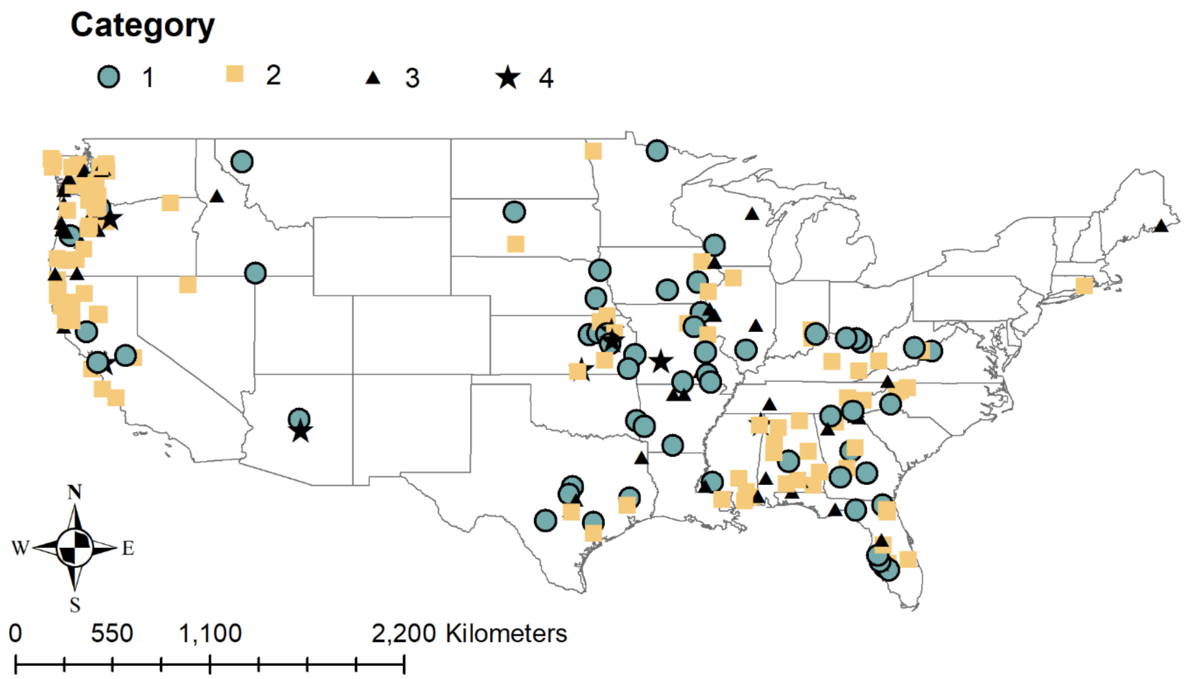

Figure 4. Recession flow predictions. **(a)** Categorization of watersheds in the CAMELS dataset based on the difference in the performance of global and GL models.

5. Potential role of watershed uniqueness and errors in model performance

The GL modeling strategy is an attempt to extract useful information from the residuals between observed and global model predicted streamflow and the useful information can only be extracted if there is some systematic structure in the residuals. A local DL model will fit the local systematic structure, but a global DL model may not fit these local structures as strongly, for example, because of averaging of the multiple structures over a large number of watersheds (Beven, 2023). The systematic structure in the residuals may either be stationary or non-stationary. Residuals dominated by both the stationary systematic structure and input-dependent nonstationary structure will contain useful information to further improve the model performance. This is because the systematic component of such a residual structure either does not change with time (stationary) or changes as a function of inputs (such as rainfall). A global model may not learn the information contained in these structures because of averaging effect or because of modeling choices, but the local part of a GL model will learn the information contained in these structures and improve the overall performance. On the other hand, the information in input-independent nonstationary structures is not learnable. A GL model will fit these structures during the training phase and perform worse (compared to the global model) in the testing phase because of the nonstationarity. Thus, we hypothesize that the GL models would improve or worsen the streamflow simulation accuracy depending upon presence or absence and stationarity or non-stationarity of residual structures.

One potential source of systematic structure in the residuals is the epistemic errors in hydrological data; the errors properties can be unique to a watershed (referred to as local errors; Beven, 2000, 2020, 2023; Gupta et al., 2023). The errors can be either pre-dominantly stationary or nonstationary. Examples of the errors include the underestimation of rainfall magnitude by rain gauges caused by the wind effect (Buttle, 1998), the consistent underestimation of areal average high rainfall volumes due to low rain gauge density (Bárdossy & Anwar, 2023) and/or rain-gauge locations (Moličová et al., 1997). Errors in rainfall timing may also occur depending on the rain-gauge locations (Gupta et al., 2023). The change in rain gauge density over time and change in rainfall spatial patterns form event to event (Austin & Houze, 1972; Over & Gupta, 1996) may introduce rainfall-independent nonstationary errors. Even if some errors are dependent upon the rainfall, available data length may not be enough to learn that dependency effectively making those errors rainfall independent (Beven, 2016). All these are the example of epistemic errors that are known to have significant influence over parameter estimation in hydrological modeling (Westerberg et al., 2011; Beven & Westerberg, 2015; Beven & Smith, 2015; Frame et al., 2023). We hypothesize that the residuals between observed and global model-predicted streamflows in a watershed exist partly due to local systematic errors, along with the effect of non-systematic errors (see Figure S4 for an illustration of systematic structure in the residuals).

Other source of systematic structure in the residuals would be watershed-specific hydrological information that could not be learnt by the global model. In case of entire hydrograph prediction, using NMAE as the objective function to train the global model (referred to as global-NMAE) resulted in better performance for some watersheds and worse performance for other watersheds (Figure S5 in SI), but overall model performance was similar to that of the global model trained using NSE as the objective function. Further, Figure S5 (SI) shows that, similar to the results shown in Figure 2, the GL model worsened the performance in most of the watersheds when outputs of the global-NMAE model were used as the input to the local part of GL models. This gives us the confidence that our conclusions regarding GL modeling are robust. The global-NMAE model significantly improved the performance compared to the global-NSE model for some of the watersheds; these are the watersheds where local models performed better than the global-NSE models. This suggests that LSTM does not extract all the relevant information from these watersheds when NSE is used as the objective function. In case of recession flow prediction, NMAE-models performed better than the NSE-models (Figure S8) but GL models still improved the performance for several watersheds (Figure S7). This suggests that it is better to train LSTM on NMAE for recession flow predictions.

Figure 2 shows that the GL models performed worse than the global model in most of the watersheds when the entire hydrograph is considered, suggesting that the residuals of the global model contained a nonstationary structure that cannot be learned by the local part of the GL models. Therefore, it suggests that the effect of systematic errors is predominantly nonstationary when the entire hydrograph is considered (see also Figure S4 in SI for an illustration of non-stationarity in residuals). This further suggests that systematic nonstationary errors is partly the reason that local DL models perform worse than the global model.

Figure 3 shows that the GL models improved the performance compared to global models in $\approx 30\%$ of the watersheds when only the recession flows were considered. This implies that a learnable structure exists in the residuals between observed and global model-predicted streamflow of these watersheds for recession flows. The GL modeling proved to be an effective strategy for recession flows (depending upon the watershed) but not for the entire hydrograph. This result may be due to the averaging of nonstationary rainfall errors when recession flows are considered since the nonstationarity of rainfall errors will more strongly impact the rising limb of the hydrograph than the recession flows.

For entire hydrograph predictions, the GL1 model performed better than GL0 model in most of the watersheds. This suggests that for most of the watersheds, there exists a relationship between the residuals and inputs (e.g., rainfall), but the relationship is too complex to be determined by the typically available length of training/calibration data (9 years in this study). In most watersheds, adding meteorological data as an input along with the global model output (GL0) degrades the full hydrograph model performance relative to only using global model output (GL1) as the input to a local model. For the recession flow predictions, GL0 did perform better than GL1 model for many of the watersheds, again suggesting the averaging of rainfall errors over a longer time-period in these watersheds.

6. Conclusions

The advent of DL models allows for extraction of predictive information about streamflow from multiple watersheds. As shown in this study, a combination of global and local modeling strategy can be applied to obtain the most accurate model for a watershed. Among different modeling strategies tested, the best modeling strategy depended upon the watershed and the portion of the hydrograph being considered. The global modeling strategy was better than other strategies for most of the watersheds in predicting the entire hydrograph. But when only the recession flows were considered, the global models were less dominant and GL models outperformed the global model for $\approx 30\%$ of the watersheds – this is a novel finding of this study. It was proposed that the performance of GL models relative to global model depends upon the nature of systematic structure in the residuals between observed and global model predicted streamflow. One of the sources of systematic structure is the epistemic errors in hydrological data. The results suggest that the errors are predominantly unlearnable and nonstationary when the entire hydrograph is considered which explains why GL models do not improve performance in this case. The nonstationary effects are likely to be averaged out when only the recession flows are considered; therefore, the GL models improve the performance compared to the global model in several watersheds in this case.

While using NMAE as the objective function instead of NSE improved performance for individual watersheds, the overall performance did not change in case of entire hydrograph prediction and the optimal configuration of the global model varies from watershed to watershed. This suggests that watershed uniqueness plays an important in global model performance and post-processing the outputs of global model by a locally trained model is a viable strategy to enhance the predictions accuracy for some watershed when only the recession flows are considered. We propose that one of the reasons the global DL model perform better than the local DL models is that local DL models may overfit the local erroneous data whereas global models with a much larger training set can generalize over data from a broad set of watersheds.

This study was limited to primarily rain-driven watersheds where it was relatively easy to identify recession limbs. A future extension of this work may employ the GL modeling strategy to snow-dominated watersheds. Further, this study used NSE and NMAE as the objective functions for DL model training, but other objective functions may be employed in future studies as different functions emphasize different parts of the hydrograph and assign different weights to training data from different watersheds.

Open Research

The data on which this article is based are available in Addor et al. (2017a, 2017b) and Newman et al. (2014, 2015).

Acknowledgments

AG was supported by the Sulo and Aileen Maki Postdoctoral Fellowship at DRI during this work. This support is gratefully acknowledged. The paper was revised several times when AG was working at the University of Cincinnati. We are grateful to Prof. Keith Beven for providing insightful comments on a draft of this paper which resulted in a better interpretation of the results presented.

References

Addor, N., Newman, A. J., Mizukami, N., & Clark, M. P. (2017a). The CAMELS data set: catchment attributes and meteorology for large-sample studies, Hydrol. Earth Syst. Sci., 21, 5293–5313, doi:10.5194/hess-21-5293-2017.

Addor, N., Newman, A. J., Mizukami, N., & Clark, M. P. (2017b). Catchment attributes for large-sample studies. Boulder, CO: UCAR/NCAR. https://doi.org/10.5065/D6G73C3Q

Ammann, L., Fenicia, F., & Reichert, P. (2019). A likelihood framework for deterministic hydrological models and the importance of non-stationary autocorrelation. Hydrology and Earth System Sciences, 23(4), 2147-2172.

Austin, P. M., & Houze, R. A. (1972). Analysis of the structure of precipitation patterns in New England. Journal of Applied Meteorology and Climatology, 11(6), 926-935.

Bárdossy, A., & Anwar, F. (2023). Why do our rainfall–runoff models keep underestimating the peak flows?. Hydrology and Earth System Sciences, 27(10), 1987-2000.

Beven, K. (2016). Facets of uncertainty: epistemic uncertainty, non-stationarity, likelihood, hypothesis testing, and communication. Hydrological Sciences Journal, 61(9), 1652-1665.

Beven, K. (2019). Towards a methodology for testing models as hypotheses in the inexact sciences. Proceedings of the Royal Society A, 475(2224), 20180862.

Beven, K. (2020). Deep learning, hydrological processes and the uniqueness of place. Hydrological Processes, 34(16), 3608-3613.

Beven, K. (2023). Benchmarking Hydrological Models for an Uncertain Future. Hydrological Processes, e14882.

Beven, K. J. (2000). Uniqueness of place and process representations in hydrological modelling. Hydrology and Earth System Sciences, 4(2), 203-213.

Beven, K. J. (2011). Rainfall-runoff modelling: the primer. John Wiley & Sons.

Beven, K., & Smith, P. (2015). Concepts of information content and likelihood in parameter calibration for hydrological simulation models. Journal of Hydrologic Engineering, 20(1), A4014010.

Beven, K., & Westerberg, I. (2011). On red herrings and real herrings: disinformation and information in hydrological inference. Hydrological Processes, 25(10), 1676-1680.

Buttle, J. M. (1998). Fundamentals of small catchment hydrology. In Isotope tracers in catchment hydrology (pp. 1-49). Elsevier.

Frame, J. M., Kratzert, F., Gupta, H. V., Ullrich, P., & Nearing, G. S. (2023). On strictly enforced mass conservation constraints for modelling the Rainfall-Runoff process. Hydrological Processes, 37(3), e14847.

Gauch, M., Mai, J., & Lin, J. (2021). The proper care and feeding of CAMELS: How limited training data affects streamflow prediction. Environmental Modelling & Software, 135, 104926.

Goodfellow, I., Bengio, Y., & Courville, A. (2016). Deep learning. MIT Press.

Govindaraju, R. S. (2000). Artificial neural networks in hydrology. I: Preliminary concepts. Journal of Hydrologic Engineering, 5(2), 115-123.

Gupta, A. (2024). Information and disinformation in hydrological data across space: The case of streamflow predictions using machine learning. Journal of Hydrology: Regional Studies, 51, 101607.

Gupta, A., Govindaraju, R. S., Li, P. C., & Merwade, V. (2023). On Constructing Limits-of-Acceptability in Watershed Hydrology using Decision Trees. Advances in Water Resources, 104486.

Kim, M., Bauser, H. H., Beven, K., & Troch, P. A. (2023). Time-Variability of Flow Recession Dynamics: Application of Machine Learning and Learning From the Machine. Water Resources Research, 59(5), e2022WR032690.

Kratzert, F., Klotz, D., Shalev, G., Klambauer, G., Hochreiter, S., & Nearing, G. (2019). Towards learning universal, regional, and local hydrological behaviors via machine learning applied to large-sample datasets. Hydrology and Earth System Sciences, 23(12), 5089-5110.

Li, X., Khandelwal, A., Jia, X., Cutler, K., Ghosh, R., Renganathan, A., ... & Kumar, V. (2022). Regionalization in a global hydrologic deep learning model: from physical descriptors to random vectors. Water Resources Research, 58(8), e2021WR031794.

Ma, K., Feng, D., Lawson, K., Tsai, W. P., Liang, C., Huang, X., ... & Shen, C. (2021). Transferring hydrologic data across continents–leveraging data-rich regions to improve hydrologic prediction in data-sparse regions. Water Resources Research, *57*(5), e2020WR028600.

Mizukami, N., Rakovec, O., Newman, A. J., Clark, M. P., Wood, A. W., Gupta, H. V., & Kumar, R. (2019). On the choice of calibration metrics for “high-flow” estimation using hydrologic models. Hydrology and Earth System Sciences, 23(6), 2601-2614.

Moličová, H., Grimaldi, M., Bonell, M., & Hubert, P. (1997). Using TOPMODEL towards identifying and modelling the hydrological patterns within a headwater, humid, tropical catchment. Hydrological Processes, 11(9), 1169-1196.

Nash, J. E., & Sutcliffe, J. V. (1970). River flow forecasting through conceptual models part I—A discussion of principles. Journal of Hydrology, 10(3), 282-290.

Nearing, G. (2014), Comment on ‘‘A blueprint for process-based modeling of uncertain hydrological systems’’ by Alberto Montanari and Demetris Koutsoyiannis, Water Resources Reseacrh, 50.

Nearing, G. S., Kratzert, F., Sampson, A. K., Pelissier, C. S., Klotz, D., Frame, J. M., ... & Gupta, H. V. (2021). What role does hydrological science play in the age of machine learning? Water Resources Research, 57(3), e2020WR028091.

Newman, A. J., Clark, M. P., Sampson, K., Wood, A., Hay, L. E., Bock, A., ... & Duan, Q. (2015). Development of a large-sample watershed-scale hydrometeorological data set for the contiguous USA: data set characteristics and assessment of regional variability in hydrologic model performance. Hydrology and Earth System Sciences, 19(1), 209-223.

Newman, A.J., Sampson, K., Clark, M. P., Bock, A., Viger, R. J., & Blodgett, D. (2014). A large-sample watershed-scale hydrometeorological dataset for the contiguous USA. Boulder, CO: UCAR/NCAR. https://dx.doi.org/10.5065/D6MW2F4D

Over, T. M., & Gupta, V. K. (1996). A space-time theory of mesoscale rainfall using random cascades. Journal of Geophysical Research: Atmospheres, 101(D21), 26319-26331.

Shen, C., & Lawson, K. (2021). Applications of deep learning in hydrology. Deep Learning for the Earth Sciences: A Comprehensive Approach to Remote Sensing, Climate Science, and Geosciences, 283-297.

Singh, V. P. (1995). Computer models of watershed hydrology. Water Resources Publications.

Smith, T., Marshall, L., & Sharma, A. (2015). Modeling residual hydrologic errors with Bayesian inference. Journal of Hydrology, 528, 29-37.

Westerberg, I. K., Guerrero, J. L., Younger, P. M., Beven, K. J., Seibert, J., Halldin, S., ... & Xu, C. Y. (2011). Calibration of hydrological models using flow-duration curves. Hydrology and Earth System Sciences, 15(7), 2205-2227.

References from supplementary information

Horner, I., Branger, F., McMillan, H., Vannier, O., & Braud, I. (2020). Information content of snow hydrological signatures based on streamflow, precipitation and air temperature. Hydrological Processes, 34(12), 2763-2779.

Kratzert, F., Klotz, D., Shalev, G., Klambauer, G., Hochreiter, S., & Nearing, G. (2019). Towards learning universal, regional, and local hydrological behaviors via machine learning applied to large-sample datasets. Hydrology and Earth System Sciences, 23(12), 5089-5110.

Lamb, R., & Beven, K. (1997). Using interactive recession curve analysis to specify a general catchment storage model. Hydrology and Earth System Sciences, 1(1), 101-113.

Tallaksen, L. M. (1995). A review of baseflow recession analysis. Journal of Hydrology, 165(1-4), 349-370

Supporting Information for

Is there Information in Residuals: Hydrograph and Recession Flows Predictions using Deep Learning?

Abhinav Gupta[1*] and Sean A. McKenna[2]

[1]Division of Hydrologic Sciences, Desert Research Institute, Las Vegas, NV
[2]Division of Hydrologic Sciences, Desert Research Institute, Reno, NV

Contents of this file

Texts S1 to S3

Figures S1 to S8

Introduction

Text S1 explains the determination of 210 watersheds used for this study. Text S2 explains the hyper-parameters tuning used in the LSTM model.

Figure S1 shows a few examples of streamflow and recession flow time series. Further, this file also contains two figures (Figures S2 and S3) which are same as figures 2 and 3 in the main text except that Kling-Gupta Efficiency (KGE) is used as the performance metric instead of Nash-Sutcliffe Efficiency (NSE).

Figure S4 shows the residuals time series between global model predicted and observed streamflow for three watersheds. Text S3 explains the Figure S4.

Text S4 contains some results for the DL models (Figures S5–S8) when NMAE was used as the objective function to train the models.

S1. Determination of recession time steps

CAMELS dataset contains data from a total of 671 basins. Out of these 671 basins, only 531 basins were used for subsequent processing following Kratzert et al. (2019c). Further, 269 basins were identified as potentially rain-driven using the criteria described in Table S1. Computation of maximum snow water equivalent (SWE) and rainfall and streamflow regimes can be found in Horner et al. (2020). For all these 269 basins, master recession curves (MRCs) were identified following Lamb and Beven (1997). Each MRC was fit with Horton's equation of baseflow recession (Tallaksen, 1995). The watersheds for which NSE between observed MRC and fitted MRC was greater than 0.95 were kept as primarily rain-driven watersheds.

Table S1. Criterion to select potentially rain-driven watersheds

	Maximum SWE	Ratio of Maximum SWE to total streamflow	Correlation between rainfall and streamflow regime
1	$< 1\text{mm}$	≤ 0.01	≥ 0.20
2	$\geq 1\text{mm}$	≤ 0.10	≥ 0.40
3	$< 10\text{mm}$	≥ 0.10	≥ 0.40
4	$\geq 10\text{mm}$	≥ 0.10	≥ 0.20
5	$\geq 1\text{mm}, \leq 10\text{mm}$	≤ 0.10	$\geq 0.20, \leq 0.40$

S2. Hyper-parameter tuning

The hyperparameter used in the global LSTM model were as follows:

(1) Sequence length (k) = 365 for full hydrograph models and 60 for recession flow models
(2) Hidden dimension: 128
(3) Number of LSTM layers = 1
(4) Learning rate = 10^{-3}
(5) Maximum number of epochs = 50
(6) Number of repetitions to account for randomness in training = 8
(7) Average prediction over 8 realizations were taken as the final prediction

The hyperparameter used in the local LSTM models were as follows:

(1) Sequence length (k) = 365 for full hydrograph models and 60 for recession flow models
(2) Hidden dimension: 128
(3) Number of LSTM layers = 1
(4) Learning rate = 10^{-3}
(5) Maximum number of epochs = 200
(6) Number of repetitions to account for randomness in training = 8
(7) Average prediction over 8 realizations were taken as the final prediction

The optimal number of epochs were decided by computing the loss on validation set after each epoch and the epoch that resulted in minimum validation loss was used the optimal epochs. This model configuration was tested in terms of reproducing the results reported by Kratzert et al. (2019); this configuration yielded NSE values almost identical to those reported by Kratzert et al. (2019) affirming that this configuration is suitable for this study. For the local and GL models, we also tried 250 epochs which resulted in either no change in NSE or an increase in NSE values by less than 0.05 for most of the watersheds; therefore, number of maximum number of epochs were limited to 200 for the local models.

The normalized mean absolute error used as objective function to train the DL models was as follows:

$$NMAE = \sum_{i=1}^{N} MAE_i/\sigma_i \quad \textbf{S1}$$

where MAE_i and σ_i are the mean absolute error and training period standard deviation of streamflow of the i^{th} watershed, and N denotes the total number of watersheds.

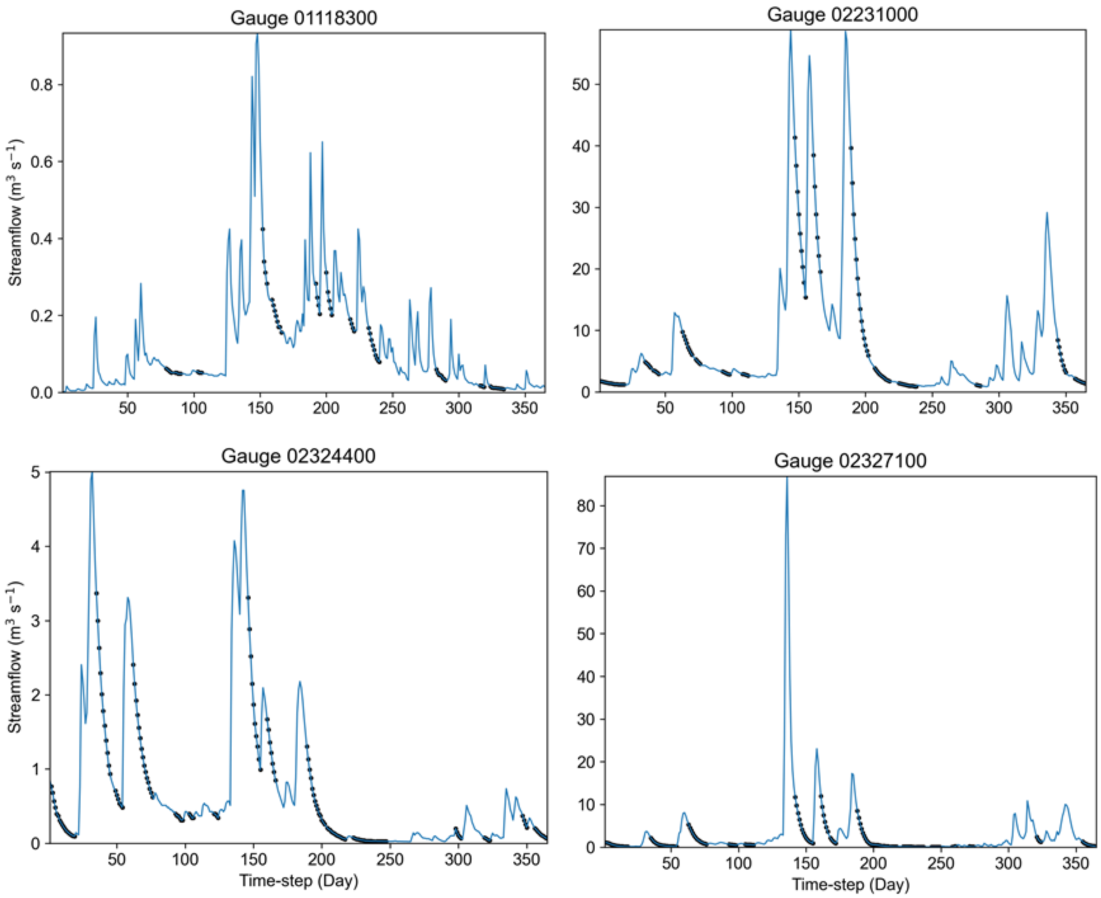

Figure S1. Streamflow time series (blue line) along with recession flow (black dots) for a watersheds

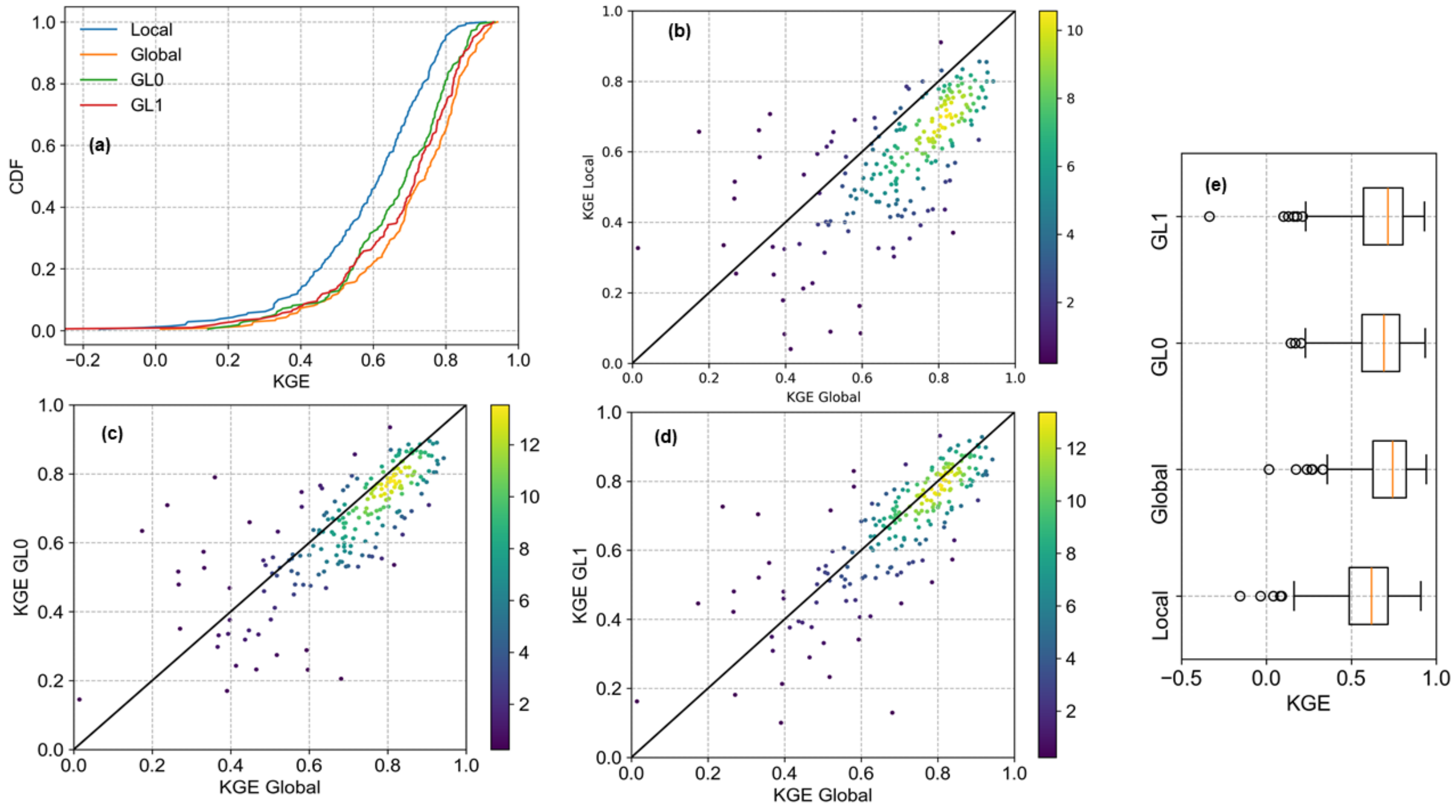

Figure S2. Entire hydrograph models. **(a)** Cumulative distribution function (CDF) of KGE values obtained by different models. The x-axis is clipped at -0.25. **(b), (c) and (d)** Comparisons of NSEs obtained by the global model to the KGEs obtained by other models; color in scatter plot represents the density of points. **(e)** Boxplots of KGE values.

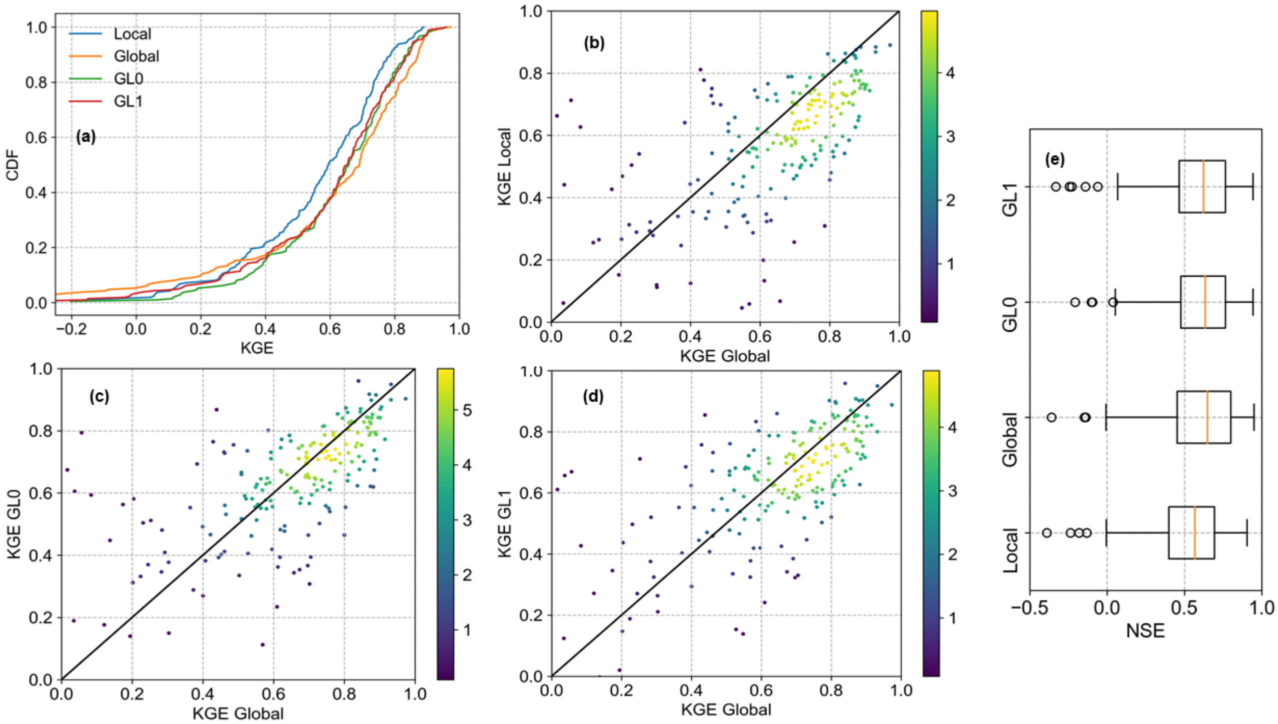

Figure S3. Recession flow models. **(a)** Cumulative distribution function (CDF) of KGEE values obtained by different models. The x-axis is clipped at -0.25. **(b), (c) and (d)** Comparisons of NSEs obtained by the global model to the KGEs obtained by other models; color in scatter plot represents the density of points. **(e)** Boxplots of KGE values.

S3. Residual structure

It is clear from Figure S4 that the residuals have a non-random systematic structure. In the Gauge 02298123, the negative residuals dominate during the first three years, but positive errors dominate for the rest of the period. Thus, a model looking at the first three years of data would not be able to learn the residual structure.

This is amplified for the Gauge 12374250, where mostly positive residuals are seen in first 5 years and then mostly negative errors are seen in the rest of the period.

In the Gauge 13083000, the global model produced positive residuals during the entire time period, but the statistical distributions of residuals between first 5 years of data and latter period are quite different, as peaks are more frequent in the latter part.

In these plots, it is also clear that GL0 model has decreased the residual magnitude at some time steps, has increase it at other time-steps.

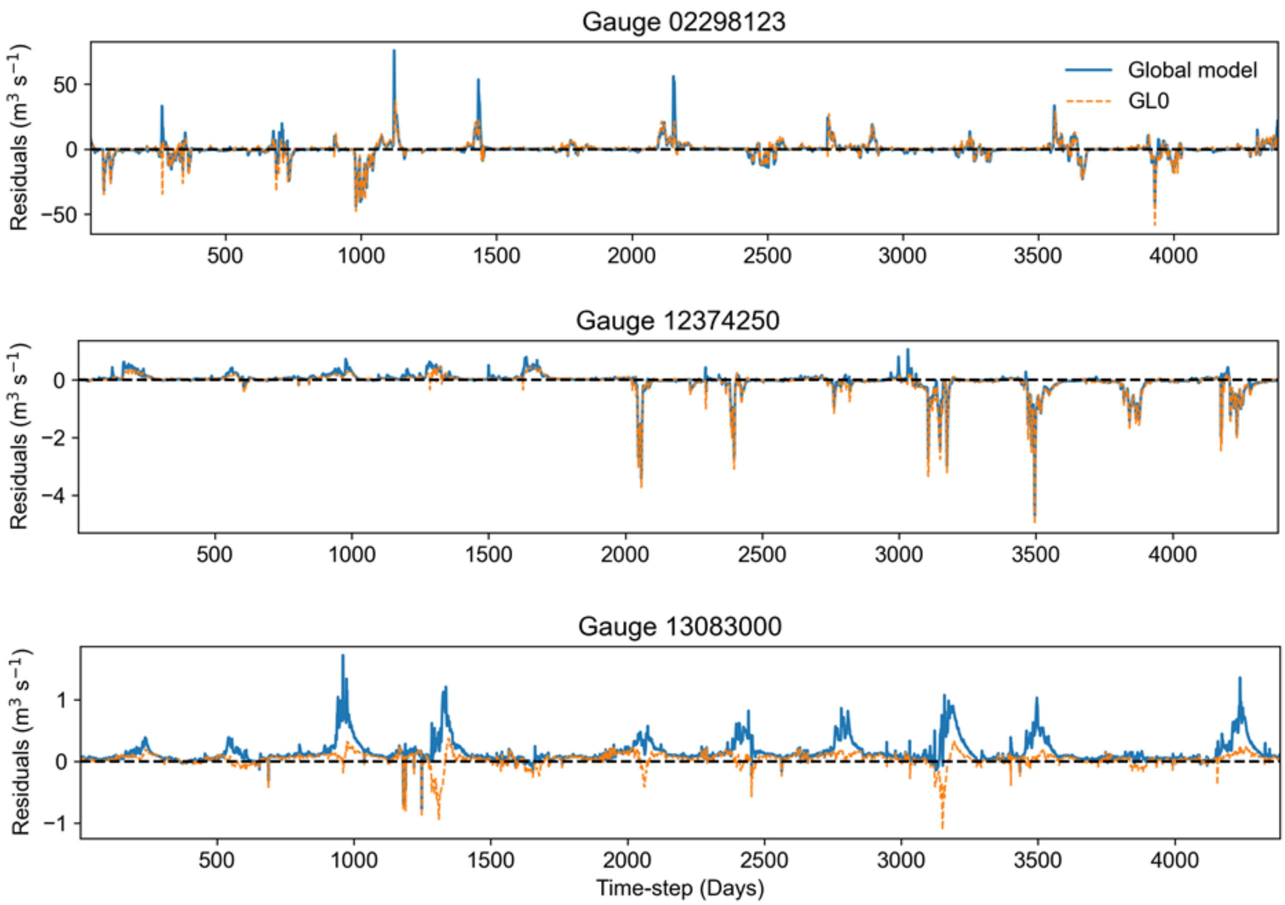

Figure S4. Residuals between observed and predicted streamflow by the global model and GL0 models for three gauges. These plots illustrate the systematic but non-stationary structure in residuals.

S4. Some results obtained using Mean Absolute Error (MAE) as objective function

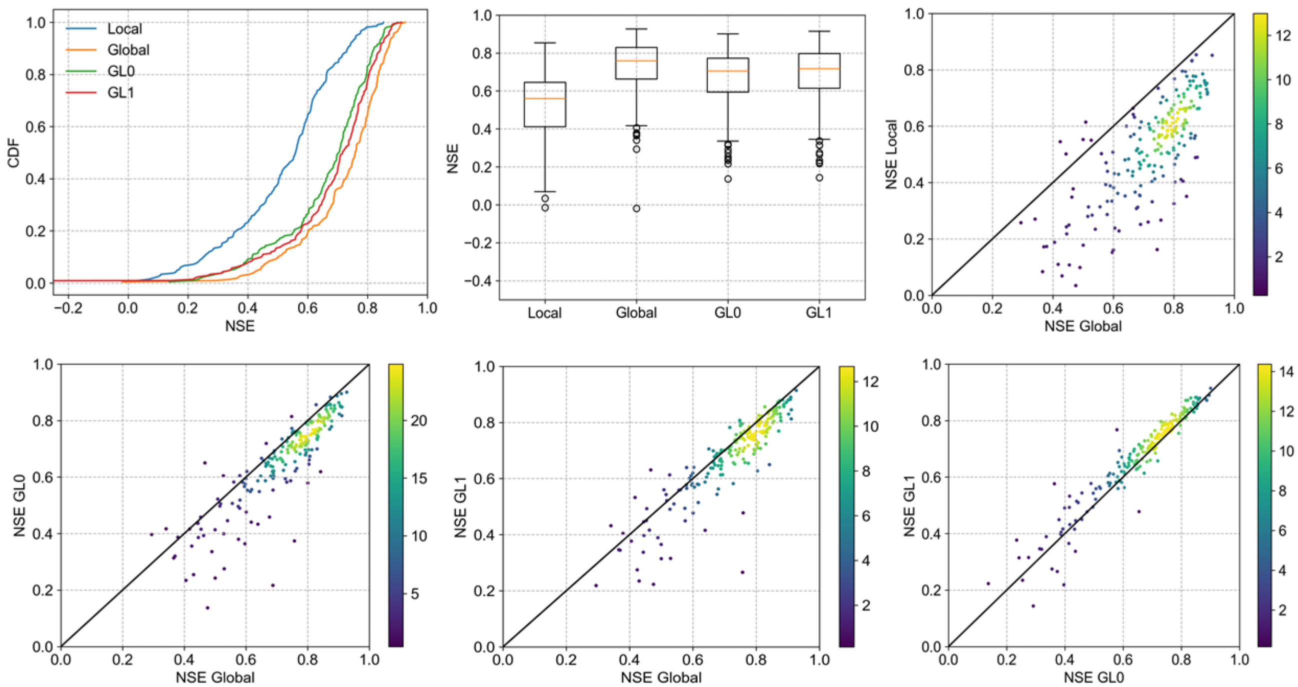

Figure S5. Entire hydrograph models but using MAE as the objective function, the local parts of GL0 and GL1 models were trained using NSE as the objective function. **(a)** Cumulative distribution function (CDF) and **(b)** boxplots of NSE values obtained by different models. As a general rule, the model with smaller area under its CDF is a better model. **(c), (d), (e), and (f)** Scatter plots of NSE values obtained by different models where x and y axes are clipped at 0.

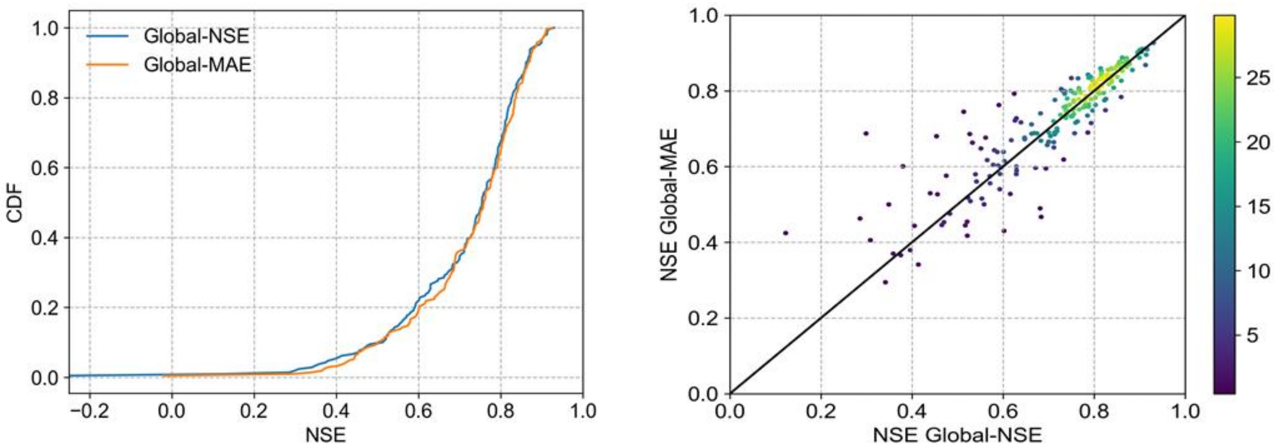

Figure S6. Entire hydrograph models. A comparison of test NSE values obtained by the global models trained using NSE and MAE as the objective functions.

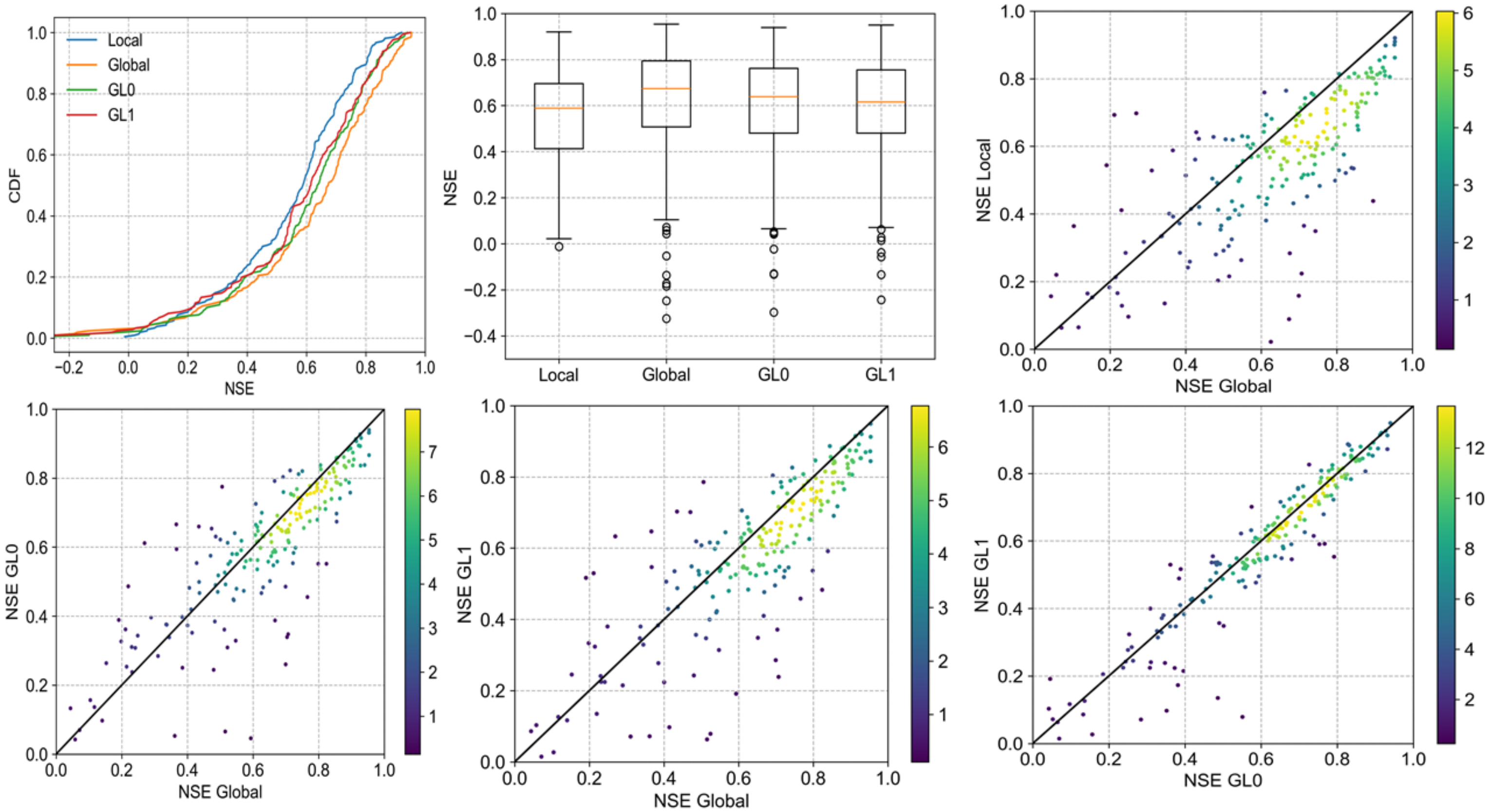

Figure S7. Recession flow models but using MAE as the objective function, the local parts of GL0 and GL1 models were trained using NSE as the objective function. **(a)** Cumulative distribution function (CDF) and **(b)** boxplots of NSE values obtained by different models. As a general rule, the model with smaller area under its CDF is a better model. **(c), (d), (e), and (f)** Scatter plots of NSE values obtained by different models where x and y axes are clipped at 0.

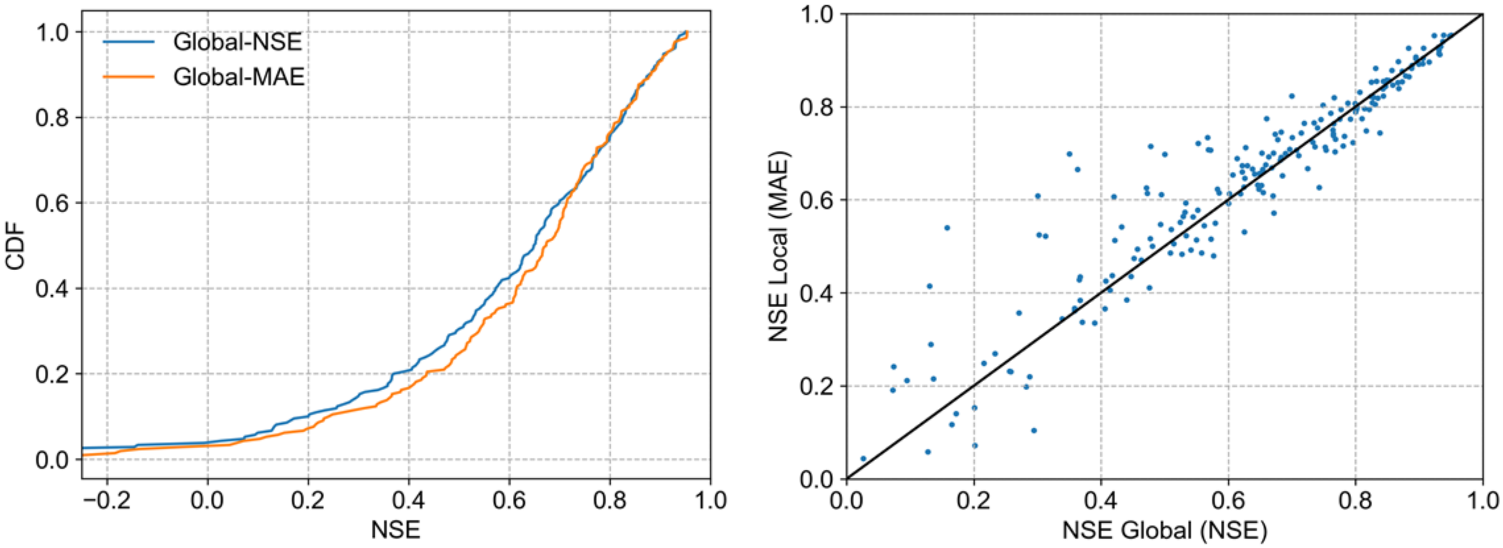

Figure S8. Recession flow models. A comparison of test NSE values obtained by the global models trained using NSE and MAE as the objective functions.